PNAS
www.pnas.org

Supplementary Information for

Targeting loss of heterozygosity for cancer-specific immunotherapy

Michael S. Hwang†, Brian J. Mog†, Jacqueline Douglass, Alexander H. Pearlman, Emily Han-Chung Hsiue, Suman Paul, Sarah R. DiNapoli, Maximilian F. Konig, Drew M. Pardoll, Sandra B. Gabelli, Chetan Bettegowda, Nickolas Papadopoulos, Bert Vogelstein, Shibin Zhou*, Kenneth W. Kinzler*

† These authors contributed equally to this work
* Corresponding authors

Contributed by Kenneth W. Kinzler

To whom correspondence should be addressed:
Email: sbzhou@jhmi.edu (S.Z.); kinzlke@jhmi.edu (K.W.K.)

This PDF file includes:

Figures S1 to S12
Tables S1 to S2
SI References

SI Figures and Tables

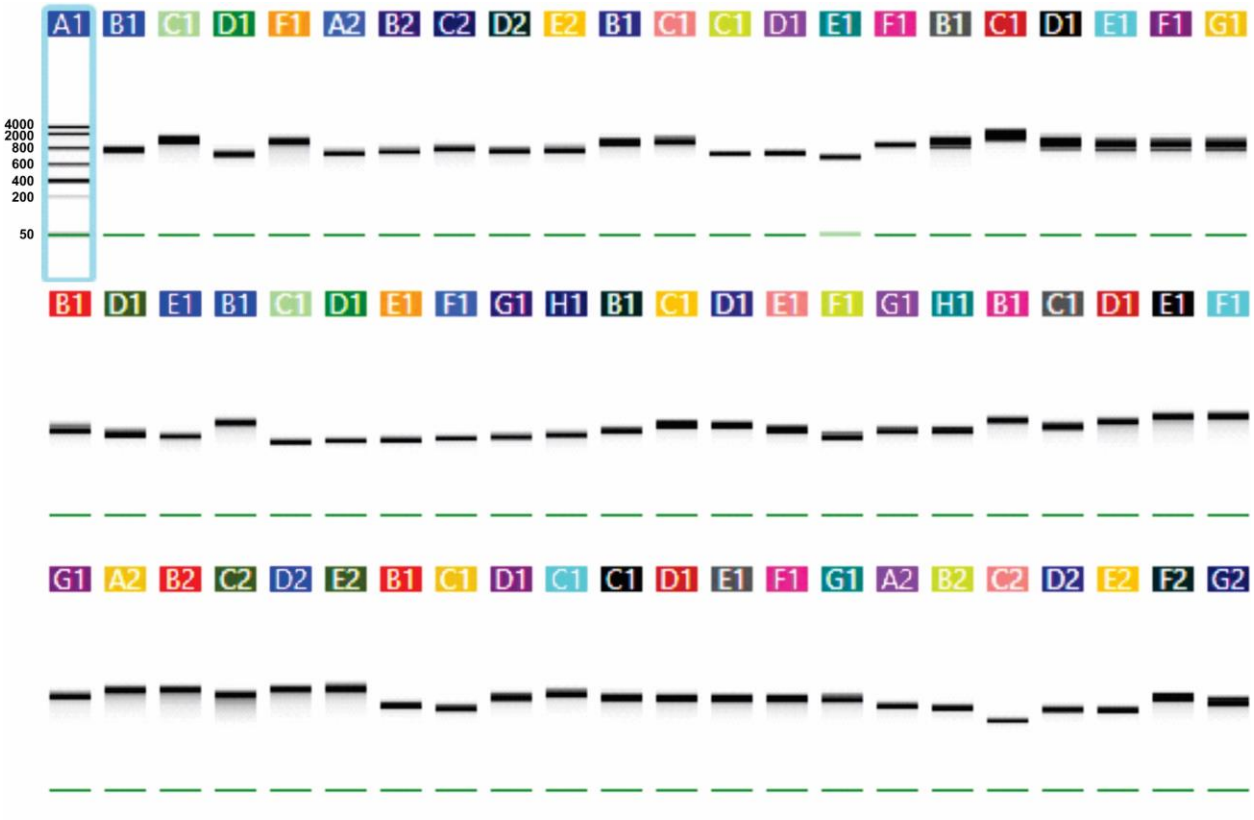

Figure S1. Robust generation of in vitro-transcribed mRNA for T-cell engineering. In this example, 65 linearized CAR plasmids were in vitro-transcribed, capped, and tailed as described in the Materials and Methods. The resultant mRNA was assessed for integrity and expected transcript size by RNA TapeStation gel analysis.

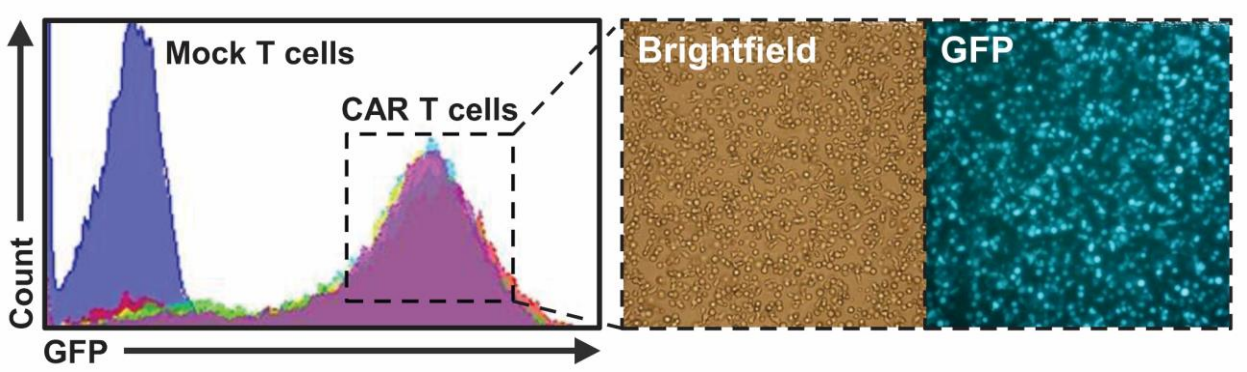

Figure S2. Efficiency of mRNA electroporation into primary human T cells. Flow cytometric evaluation of primary human T cells following CAR mRNA electroporation. Five unique CAR mRNAs were electroporated into T cells, while Mock indicates T cells electroporated with no mRNA. *Inset*, representative brightfield and fluorescent images of T cells following CAR mRNA electroporation. GFP fluorescence was used to assess transfection efficiency.

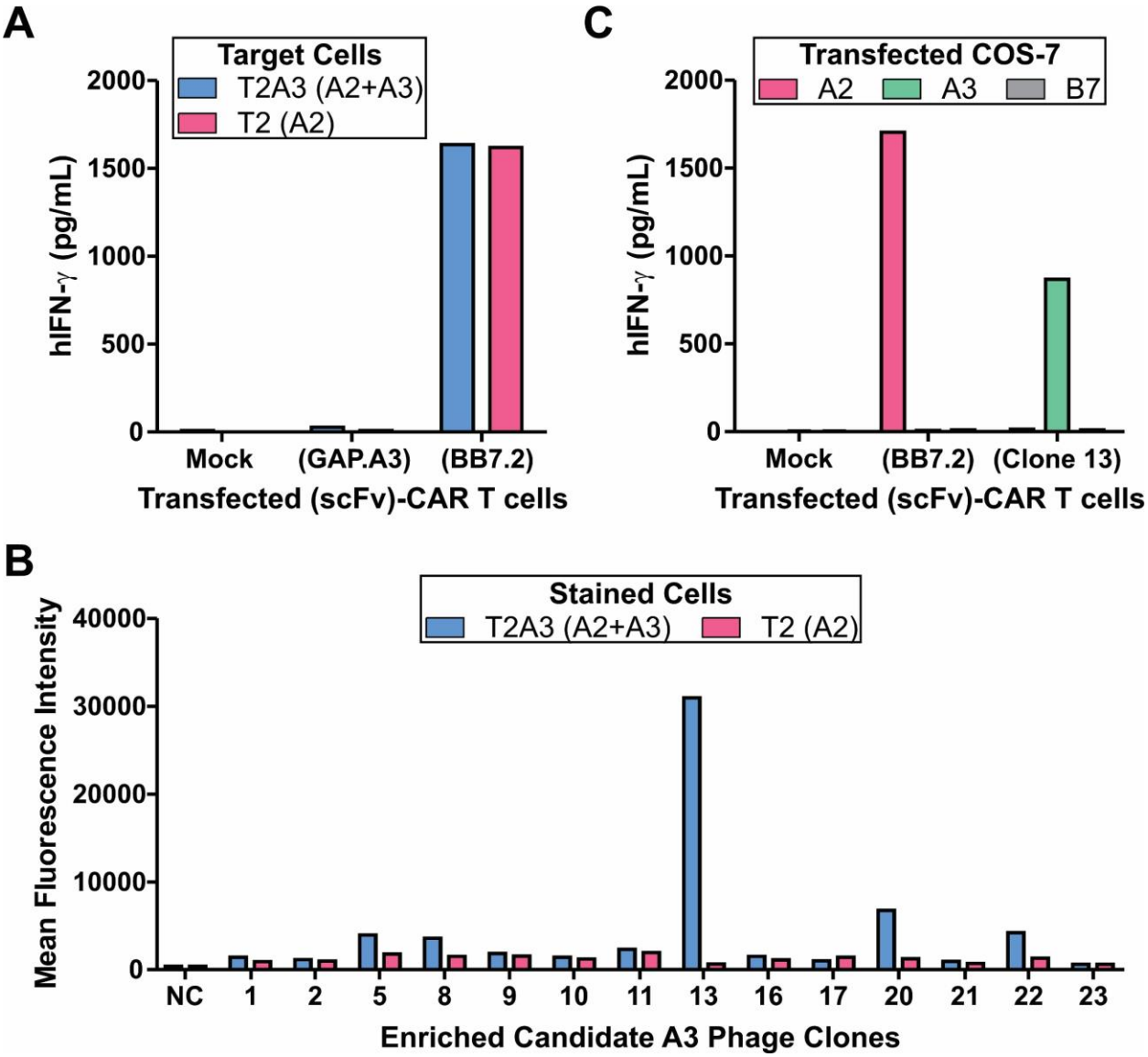

Figure S3. Identification of HLA-A3 allele-specific scFvs with phage display technology. (A) T cells expressing a CAR grafted with either a GAP.A3 (α-A3) or BB7.2 (α-A2) scFv were co-incubated with target cell lines expressing A2 and A3 (T2A3) or A2 only (T2). T-cell activation was assessed by ELISA for secreted IFN-γ. Data are representative of two independent experiments demonstrating the same trend in response. (B) Following panning, enriched candidate A3 phage clones were evaluated for binding to cell lines expressing A2 and A3 (T2A3 cells) or A2 only (T2 cells) by flow cytometry. NC, no phage control. (C) T cells expressing a CAR grafted with either a BB7.2 (α-A2) or Clone 13 (α-A3) scFv were co-incubated with COS-7 cells transfected with the indicated *HLA-A* or *HLA-B* allele at an E:T ratio of 1:1. T-cell activation was assessed by ELISA for secreted IFN-γ. Data are representative of four independent

experiments demonstrating the same trend in response. In addition, similar results were obtained in separate experiments with *HLA* KO isogenic cancer cell lines and when employing constructs containing fluorophores (e.g. GFP, mCherry).

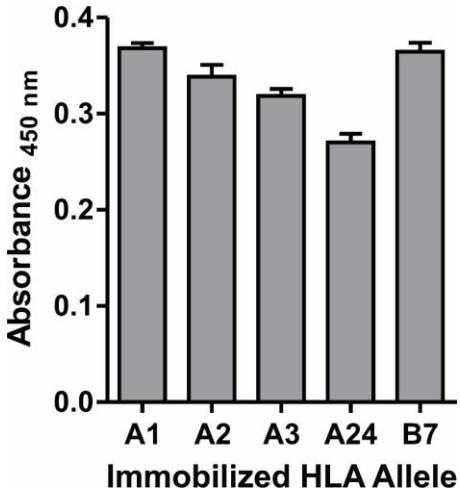

Figure S4. Evaluation of pHLA antigen integrity. pHLA complexes were evaluated for antigen integrity by performing an ELISA using the W6/32 antibody, which recognizes only folded HLA. Data represent means ± SD of three technical replicates.

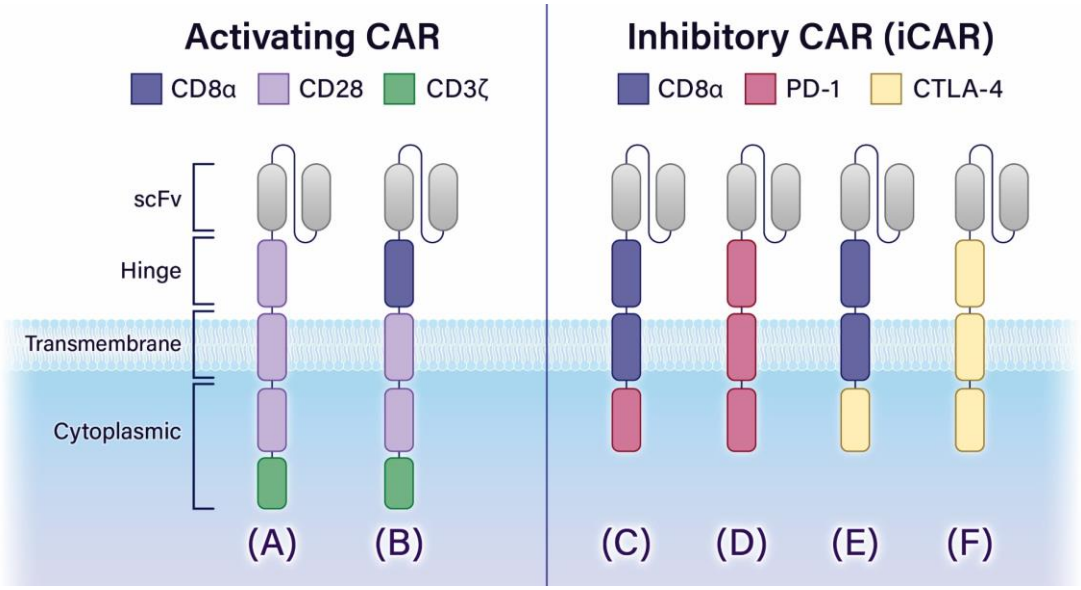

Figure S5. CAR and iCAR design illustrations. A summary of the CAR and iCAR designs employed during NASCAR optimization. (A) CD28-hinged 2nd generation CAR. (B) CD8α-hinged 2nd generation CAR. (C) PD-1 cytoplasmic domain with CD8α hinge and transmembrane domain iCAR. (D) PD-1 cytoplasmic domain with endogenous PD-1 hinge and transmembrane domain iCAR. (E) CTLA-4 cytoplasmic domain with CD8α hinge and transmembrane domain iCAR. (F) CTLA-4 cytoplasmic domain with endogenous CTLA-4 hinge and transmembrane domain iCAR.

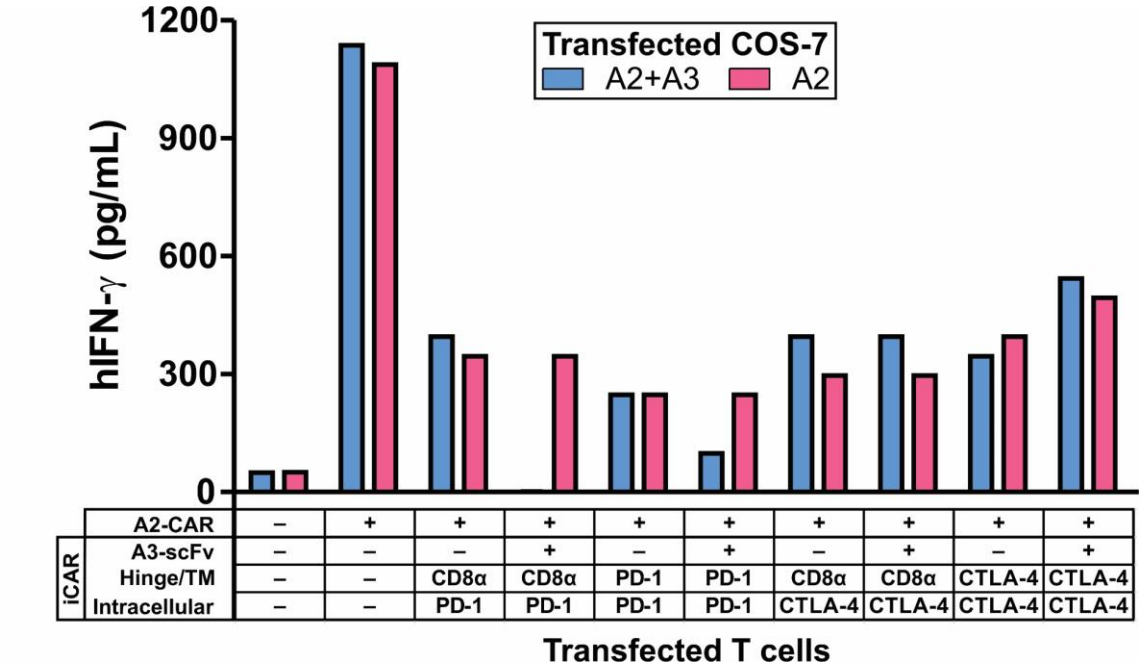

Figure S6. NASCAR inhibitory module optimization. T cells configured with the indicated CAR and variant iCAR combinations were co-incubated with COS-7 cells transfected with the indicated *HLA-A* allele(s) at an E:T ratio of 1:1. T-cell activation was assessed by ELISA for secreted IFN-γ. Data are representative of three independent experiments demonstrating the same trend in response. In addition, similar results were obtained in separate experiments when the mirrored combination of CAR and iCAR (e.g. A3-CAR, A2-iCAR) was tested and when employing constructs containing fluorophores (e.g. GFP, mCherry). TM, transmembrane.

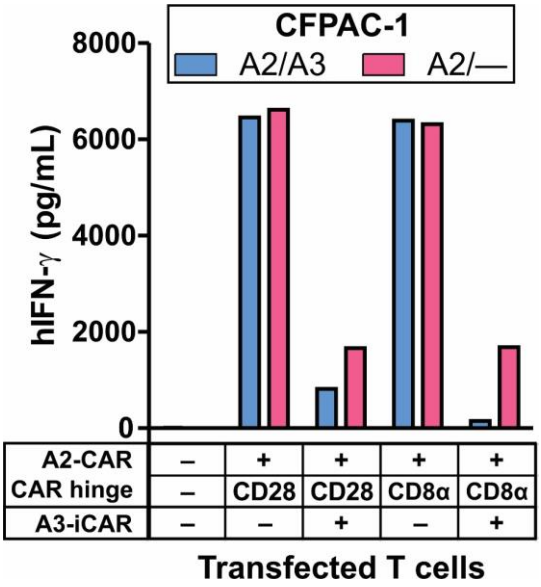

Figure S7. NASCAR activating module optimization. T cells configured with the indicated hinge variant CAR and iCAR combinations were co-incubated with CFPAC-1 *HLA* KO isogenic cell lines with the indicated HLA-A allele status at an E:T ratio of 1:1. T-cell activation was assessed by ELISA for secreted IFN-γ. Data are representative of four independent experiments demonstrating the same trend in response tested in two separate donors. In addition, similar results were obtained in separate experiments employing constructs containing fluorophores (e.g. GFP, mCherry).

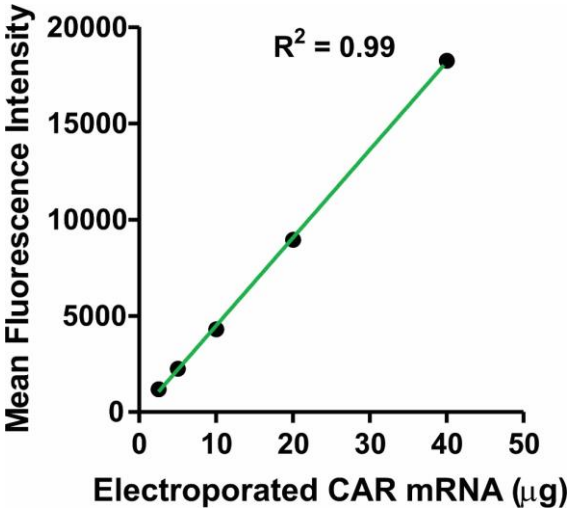

Figure S8. Correlation between electroporated mRNA and CAR expression. The indicated amounts of CAR mRNA were electroporated into primary human T cells. CAR expression, as assessed by GFP levels, was evaluated by flow cytometry.

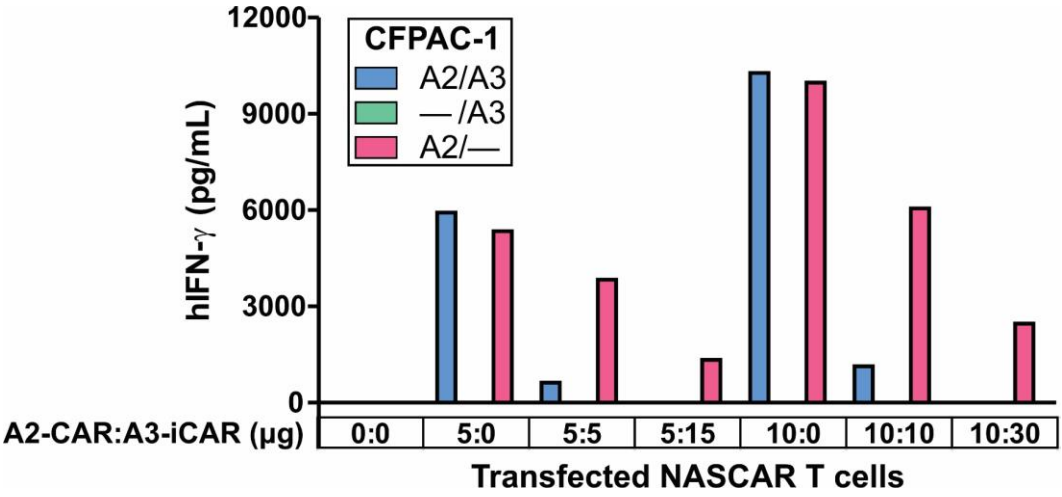

Figure S9. NASCAR stoichiometric optimization for allele-specific inhibition. T cells configured with the indicated amounts and ratios of CAR and iCAR were co-incubated with CFPAC-1 *HLA* KO isogenic cell lines with the indicated HLA-A allele status at an E:T ratio of 1:1. T-cell activation was assessed by ELISA for secreted IFN-γ. Data are representative of three independent experiments demonstrating the same trend in response. In addition, similar results were obtained in separate experiments employing constructs containing fluorophores (e.g. GFP, mCherry).

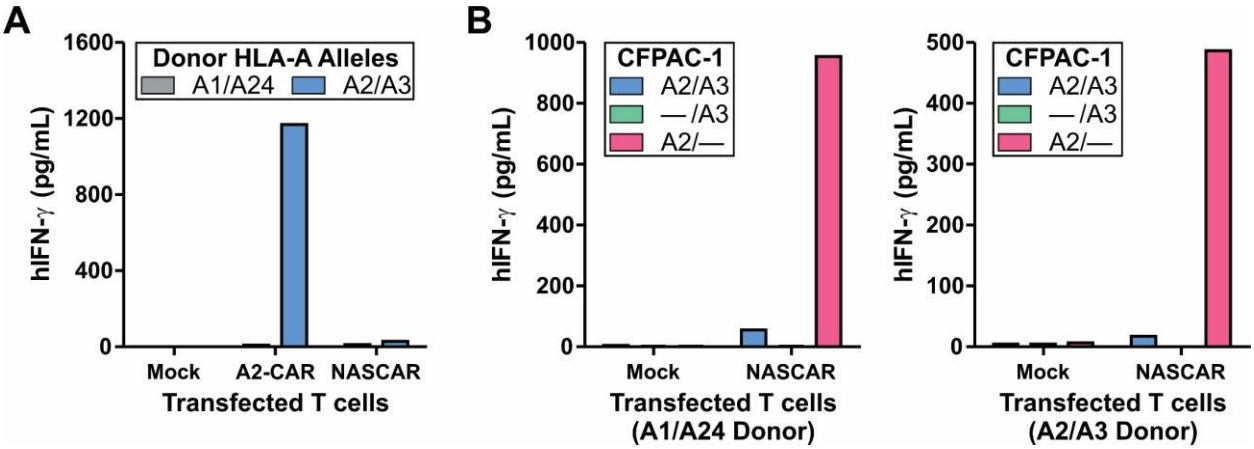

Figure S10. Assessment of NASCAR autoreactivity and re-challenge in "autologous" T cells. (A) A2-CAR T cells or NASCAR T cells targeting A3 loss from two different donors with the indicated HLA-A alleles were independently cultured. T-cell autoreactivity was assessed by ELISA for secreted IFN-γ. Data are representative of three independent experiments demonstrating the same trend in response. (B) A2-CAR T cells or NASCAR T cells targeting A3 loss from two different donors with the indicated HLA-A alleles were co-incubated with CFPAC-1 *HLA* KO isogenic cell lines with the indicated HLA-A allele status at an E:T ratio of 1:1. T-cell activation, upon re-challenge to CFPAC-1 target cells, was assessed by ELISA for secreted IFN-γ. Data are representative of three independent experiments demonstrating the same trend in response.

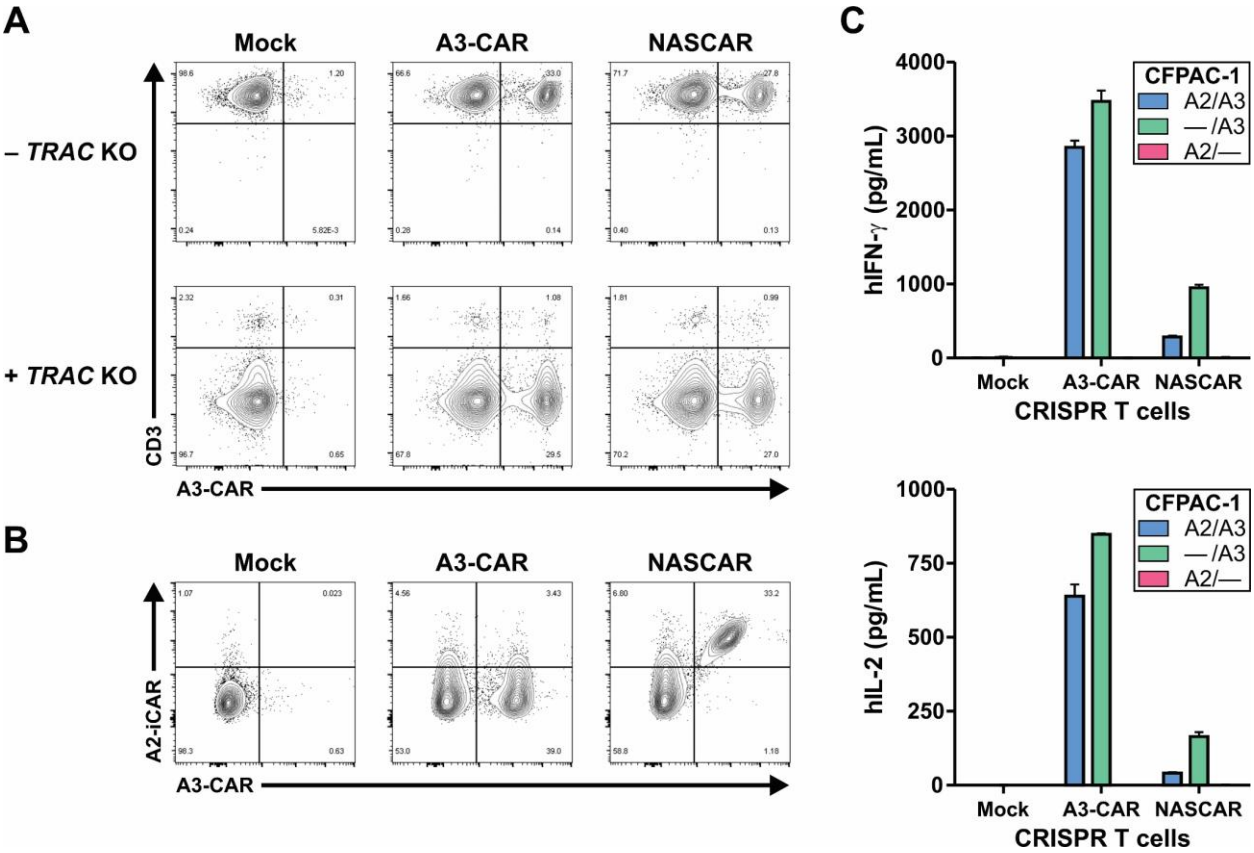

Figure S11. Generation and allele-specificity of CRISPR-engineered NASCAR T cells. (A) Flow cytometric evaluation with Protein L and α-CD3 antibody of CRISPR-engineered A3-CAR T cells or NASCAR T cells targeting A2 loss following knock-in of the indicated expression cassette at the *B2M* locus, with or without simultaneous *TRAC* KO. (B) Flow cytometric evaluation with A2 or A3 pHLA tetramers of CRISPR-engineered A3-CAR T cells or NASCAR T cells targeting A2 loss following knock-in of the indicated expression cassette at the *B2M* locus with simultaneous *TRAC* KO. (C) CRISPR-engineered A3-CAR T cells or NASCAR T cells targeting A2 loss were co-incubated with CFPAC-1 *HLA* KO isogenic cell lines with the indicated HLA-A allele status at an editing efficiency-corrected E:T ratio of 1:1. T-cell activation was assessed by ELISA for secreted IFN-γ (top) and IL-2 (bottom). Data represent means ± SD of two technical replicates.

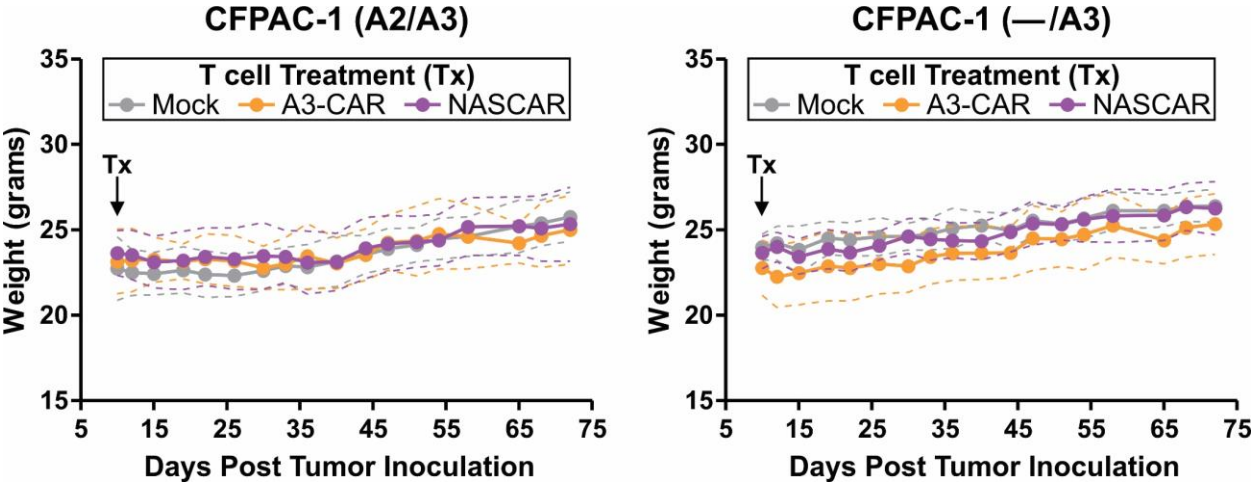

Figure S12. Body weight assessment of subcutaneous xenograft tumor model. A single-flank, subcutaneous xenograft model of NSG mice was employed, and CRISPR-engineered A3-CAR T cells and NASCAR T cells targeting A2 loss were introduced via tail vein IV injection 10 days following tumor inoculation. Body weights of the mice were serially monitored throughout the duration of the 75-day experiment. N = 6 mice per group. Data represent means ± SD.

Table S1. Frequencies of chromosome 6p LOH in cancer.

Cancer Type	Reported 6p Arm Loss	Reference
Bladder	35%	*(96)*
Breast	24%	*(98)*
	27%	*(126)*
Cervical	68%	*(91)*
Colon	13.8%	*(89)*
	25%	*(19)*
	40%	*(96)*
Glioblastoma	41.4%	*(97)*
Laryngeal	17.6%	*(89)*
	53%	*(96)*
Lung	40%	*(93)*
	41%	*(95)*
Melanoma	15.3%	*(89)*
	23%	*(96)*
Ovarian	28%	*(127)*
Pancreas	50%	*(94)*
Renal	6%	*(96)*

Reported frequencies of chromosome 6p LOH across various cancer types; cancer type denoted in left column, 6p LOH frequency in center column, and corresponding reference in right column (*96*, *98*, *126*, *91*, *89*, *19*, *97*, *93*, *95*, *127*, *94*).

Table S2. Authentication of *HLA* KO isogenic target cell lines.

Query Name	Top Matches	Match %	TH01	D5S818	D13S317	D7S820	D16S539	CSF1PO	vWA	TPOX
CFPAC-1 (A2/A3)	CFPAC-1 [CRL-1918]	100	8	10, 11	12	8, 10	9, 11	10	17	8
CFPAC-1 (— /A3)	CFPAC-1 [CRL-1918]	100	8	10, 11	12	8, 10	9, 11	10	17	8
CFPAC-1 (A2/—)	CFPAC-1 [CRL-1918]	100	8	10, 11	12	8, 10	9, 11	10	17	8
NCI-H441 (A2/A3)	NCI-H441 [HTB-174]	100	9.3	11, 12	9	10	9, 13	11, 12	17	8, 10
NCI-H441 (— /A3)	NCI-H441 [HTB-174]	100	9.3	11, 12	9	10	9, 13	11, 12	17	8, 10
NCI-H441 (A2/—)	NCI-H441 [HTB-174]	100	9.3	11, 12	9	10	9, 13	11, 12	17	8, 10
RPMI-6666 LucGFP (A2/A3)	RPMI-6666 [CCL-113]	100	6, 9	11, 12	11	9, 10	11, 12	12, 13	14, 18	10, 11
RPMI-6666 LucGFP (— /A3)	RPMI-6666 [CCL-113]	100	6, 9	11, 12	11	9, 10	11, 12	12, 13	14, 18	10, 11
RPMI-6666 LucGFP (A2/—)	RPMI-6666 [CCL-113]	100	6, 9	11, 12	11	9, 10	11, 12	12, 13	14, 18	10, 11

Final *HLA* KO isogenic clones were subject to STR profiling. Eight core STR loci were tested, and the top profile match in the ATCC STR database, along with match percentage, is displayed.

SI References

19. B. Vogelstein, E. R. Fearon, S. E. Kern, S. R. Hamilton, A. C. Preisinger, Y. Nakamura, R. White, Allelotype of colorectal carcinomas. *Science*. **244**, 207–211 (1989).

89. P. Jiménez, J. Cantón, A. Collado, T. Cabrera, A. Serrano, L. M. Real, A. García, F. Ruiz-Cabello, F. Garrido, Chromosome loss is the most frequent mechanism contributing to HLA haplotype loss in human tumors. *International Journal of Cancer*. **83**, 91–97 (1999).

91. N. N. Mazurenko, I. S. Beliakov, A. Yu. Bliyev, Z. Guo, X. Hu, S. V. Vinokourova, B. A. Bidzhieva, L. S. Pavlova, J. Ponten, F. L. Kisseljov, Genetic Alterations at Chromosome 6 Associated with Cervical Cancer Progression. *Molecular Biology*. **37**, 404–411 (2003).

93. N. McGranahan, R. Rosenthal, C. T. Hiley, A. J. Rowan, T. B. K. Watkins, G. A. Wilson, N. J. Birkbak, S. Veeriah, P. Van Loo, J. Herrero, C. Swanton, Allele-Specific HLA Loss and Immune Escape in Lung Cancer Evolution. *Cell*. **171**, 1259-1271.e11 (2017).

94. S. A. Hahn, A. B. Seymour, Allelotype of Pancreatic Adenocarcinoma Using Xenograft Enrichment, 7.

95. L. Girard, S. Zöchbauer-Müller, A. K. Virmani, A. F. Gazdar, J. D. Minna, Genome-wide Allelotyping of Lung Cancer Identifies New Regions of Allelic Loss, Differences between Small Cell Lung Cancer and Non-Small Cell Lung Cancer, and Loci Clustering. *Cancer Res*. **60**, 4894–4906 (2000).

96. I. Maleno, N. Aptsiauri, T. Cabrera, A. Gallego, A. Paschen, M. A. López-Nevot, F. Garrido, Frequent loss of heterozygosity in the β2-microglobulin region of chromosome 15 in primary human tumors. *Immunogenetics*. **63**, 65–71 (2011).

97. J. T. Yeung, R. L. Hamilton, K. Ohnishi, M. Ikeura, D. M. Potter, M. N. Nikiforova, S. Ferrone, R. I. Jakacki, I. F. Pollack, H. Okada, LOH in the HLA Class I region at 6p21 is Associated with Shorter Survival in Newly Diagnosed Adult Glioblastoma. *Clin Cancer Res*. **19**, 1816–1826 (2013).

98. M. A. Garrido, T. Rodriguez, S. Zinchenko, I. Maleno, F. Ruiz-Cabello, Á. Concha, N. Olea, F. Garrido, N. Aptsiauri, HLA class I alterations in breast carcinoma are associated with a high frequency of the loss of heterozygosity at chromosomes 6 and 15. *Immunogenetics*. **70**, 647–659 (2018).

126. F. Lerebours, P. Bertheau, I. Bieche, K. Driouch, H. de The, K. Hacene, M. Espie, M. Marty, R. Lidereau, Evidence of chromosome regions and gene involvement in inflammatory breast cancer. *International Journal of Cancer*. **102**, 618–622 (2002).

127. W. D. Foulkes, J. Ragoussis, G. W. H. Stamp, G. J. Allan, J. Trowsdale, Frequent loss of heterozygosity on chromosome 6 in human ovarian carcinoma. *British Journal of Cancer*. **67**, 551–559 (1993).